Applied Surface Science 276 (2013) 7–12

Contents lists available at SciVerse ScienceDirect

Applied Surface Science

journal homepage: www.elsevier.com/locate/apsusc

Characterization of CuO(1 1 1)/MgO(1 0 0) films grown under two different PLD backgrounds

M. Kawwam [a,b,*], F.H. Alharbi [c,d], T. Kayed [f], A. Aldwayyan [b], A. Alyamani [c], N. Tabet [e], K. Lebbou [a]

[a] Laboratoire de Physico Chimie des Matériaux Luminescents (LPCML) UMR 5620 CNRS Université de Lyon 1, 69622 Villeurbanne cedex, Lyon, France
[b] King Abdullah Institute for Nanotechnology, King Saud University, Riyadh, Saudi Arabia
[c] Energy Research Institute, King Abdulaziz City for Science and Technology (KACST), Riyadh, Saudi Arabia
[d] Qatar Environment & Energy Research Institute, Doha, Qatar
[e] King Fahd University of Petroleum and Minerals, Dhahran, Saudi Arabia
[f] College of Engineering University of Dammam, Saudi Arabia

ARTICLE INFO

Article history:
Received 10 January 2013
Received in revised form 11 February 2013
Accepted 12 February 2013
Available online 22 March 2013

Keywords:
CuO/MgO
PLD
Pulsed laser deposition
Thin film
Optoelectronic
Background

ABSTRACT

Cupric oxide (CuO) films were deposited on MgO (1 0 0) substrates by two different pulsed laser deposition (PLD) configurations, molecular gas background and RF-plasma assisted, at temperatures over 250–450 °C range. The films were characterized by X-ray diffraction (XRD), reflection of high energy electron diffraction (RHEED), X-ray photoelectron spectroscopy (XPS), atomic force microscopy (AFM), ellipsometery, and four probe conductivity measurements. The heating temperature was found to have a limited effect on the structural properties of the films grown in RF-plasma assisted background while it has a significant effect in the case of the standard gas background. The structural observations revealed that RF-plasma background increased the possibility of Frank–van der Merwe or the initial stages of Stranski–Krastanov growth mode, leaving the CuO films highly textured in (1 1 1) direction, atomically smooth and chemically stoichiometric. Optoelectronic properties of best obtained CuO film are presented as well.

© 2013 Elsevier B.V. All rights reserved.

1. Introduction

Cupric oxide (CuO) has attracted more interest as a promising material for solar energy devices due to the matching optical and electrical properties [1] and due to its low thermal emittance [2]. It is an indirect band gap semiconductor with about 1.4 eV Eg. The smallest direct transition starts at 1.7 eV [3]. Furthermore, it is expected that it would be an inexpensive cell as the constituent materials are abundantly available on earth crust. CuO is known to be p-type semiconductor mainly due to the presence of negatively charged copper vacancies in the structure which act as acceptors. It has been utilized in photovoltaic devices [4,5], pn junction diodes [6], power sources [5,7], microwave dielectrics [8], solid state gas sensor [9,10], and catalysts for several environmental processes [11,12]. CuO thin films have been grown by a variety of preparation techniques like thermal oxidation [13–15], electrodeposition [16], molecular beam epitaxy [17], induced physical vapor deposition [18,19], radio frequency magnetron sputtering [20], and pulsed laser deposition [21–23]. Many of the above reports studied the structural, optical and electrical properties of CuO films; few of them discussed the effect of activating the process background.

Despite the large differences in structure and symmetry between both materials, the growth of CuO on MgO is shown to be polycrystalline and strongly textured in (1 1 1) direction parallel to the (0 0 1) MgO planes [17,24]. In previous report, the growth of CuO films on different substrates (MgO (1 0 0), STO (1 0 0), Sapphire (0 0 0 1), and Quartz (0 0 0 1)) using PLD were studied [25]. Based on explained results, MgO (1 0 0) was selected for a systematic investigation of the morphology of CuO surface as a function of PLD parameters (temperature, pressure, working distance, and laser fluence). As a final result of our previous work [25], we have been able to minimize the average surface roughness and the density and size of liquid micro-droplets found on surfaces. In this work, a comparison between two different PLD configurations to grow single phase crystalline CuO films on MgO is presented. At different heating temperatures, the first configuration utilized a radio-frequency source to generate an active oxygen atmosphere while the other operated in molecular oxygen background. The aim of this approach is to investigate the effect of R.F. Plasma which activates the process background during ablation, perhaps allowing the growth of films of better structural and optoelectronic properties.

* Corresponding author. Tel.: +33 96170605605.
E-mail address: Mohammad.kawwam@univ-lyon1.fr (M. Kawwam).

0169-4332/$ – see front matter © 2013 Elsevier B.V. All rights reserved.
http://dx.doi.org/10.1016/j.apsusc.2013.02.051

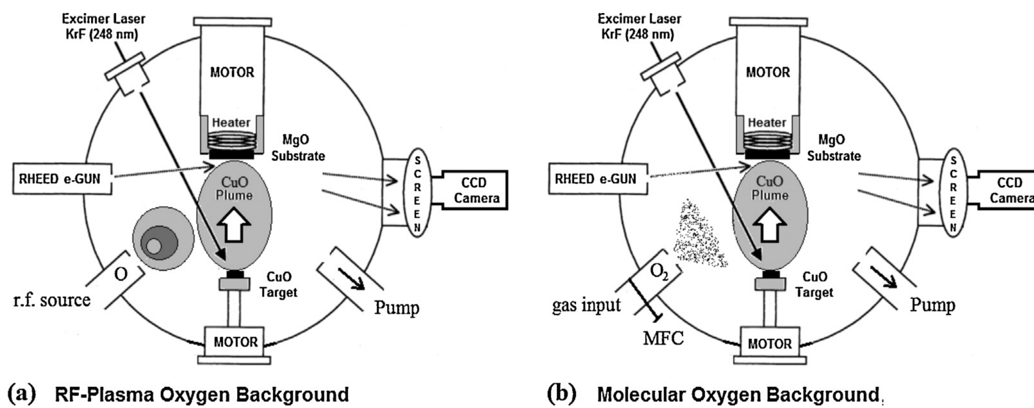

Fig. 1. Two different PLD configurations, (a) R.F. plasma assisted background, (b) molecular gas background.

2. Experimental details

The CuO thin films were deposited on MgO (1 0 0) substrates using typical PLD setup, shown schematically in Fig. 1, in two different configurations: (i) using the oxygen radical beam source (R.F. excited at 13.6 MHz and 400 W) (Fig. 1a), (ii) purging (99.999% purity) oxygen gas through mass flow controller (Fig. 1b). All PLD parameters which may contribute to growth rate were kept constant and the film thickness measured by Stylus Profiler (Veeco Dektak 150) was kept: 100–120 nm for all samples. For both configurations the background pressure was kept at 12×10^{-3} Pa while the substrate temperature varied from 250 °C to 450 °C. The films will be used later to develop CuO-based solar cells. So, growing good quality films at relatively low temperature is one of the main goals. Prior to deposition, MgO substrates were degassed at 850 °C while the chamber was pumped down to 10^{-8} Pa. KrF excimer laser (COMPex Pro 205, λ = 248 nm, pulse width = 20 ns, and repetition rate = 15 Hz) was operated at 1.0 J/cm^2 to ablate a commercial CuO target (99.99% from MTI Corp.). The laser beam was focused on the target at 45° incidence angle through a converging lens (f = 500 mm) and a UV-grade quartz port window. To avoid fast drilling, the target was mounted onto a rotating and spinning holder. The single crystal MgO (1 0 0) substrates were put also onto a rotating holder in an off-axis position with respect to the CuO plume normal and 125 mm from the target.During the CuO film deposition, the growth modes were monitored by in situ high-pressure reflection high-energy electron diffraction (RHEED) [KSA400]. A 20 keV electron beam with an incidence angle of around 1° was directed along [1–9] azimuth.

The RHEED diffraction patterns and intensity profiles in specular reflection geometry were recorded at deposition rate of 2 Hz using a charge-coupled device camera with acquisition software (K-Space Associates). After deposition, the film thickness profiles were monitored by Stylus Profiler (VeecoDektak 150). The surface morphology

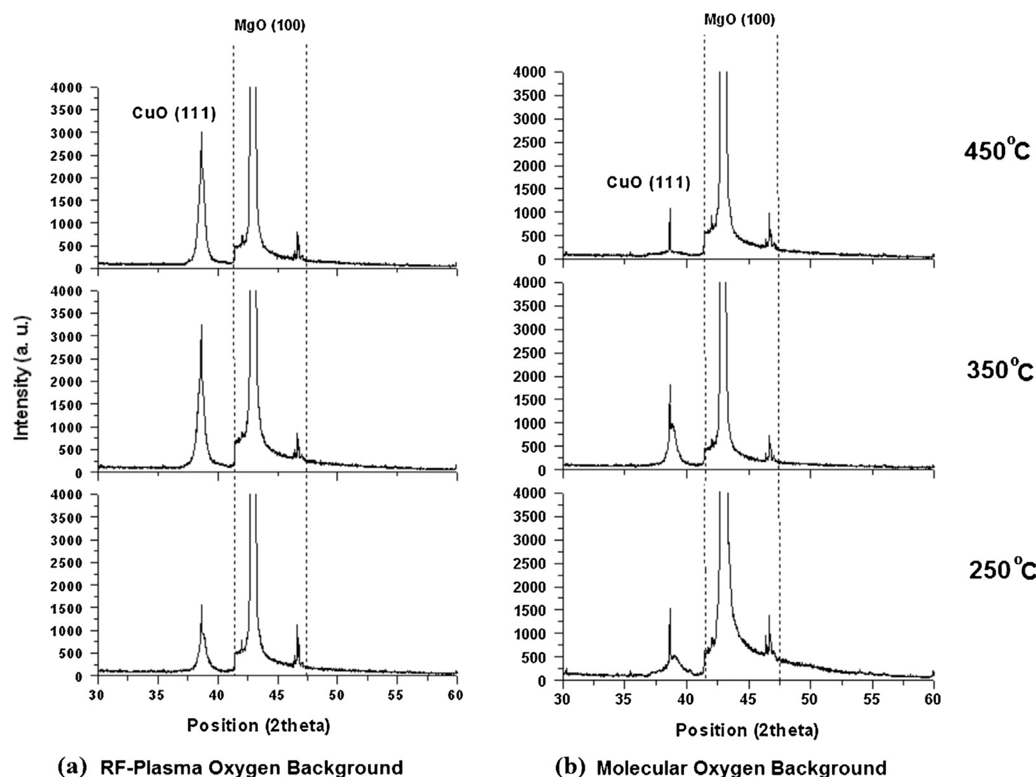

Fig. 2. Typical XRD (θ–2θ) scans for PLD grown CuO films, as a function of substrate temperature (250–450 °C) using two different PLD configurations, (a) R.F. plasma assisted background, (b) molecular gas background.

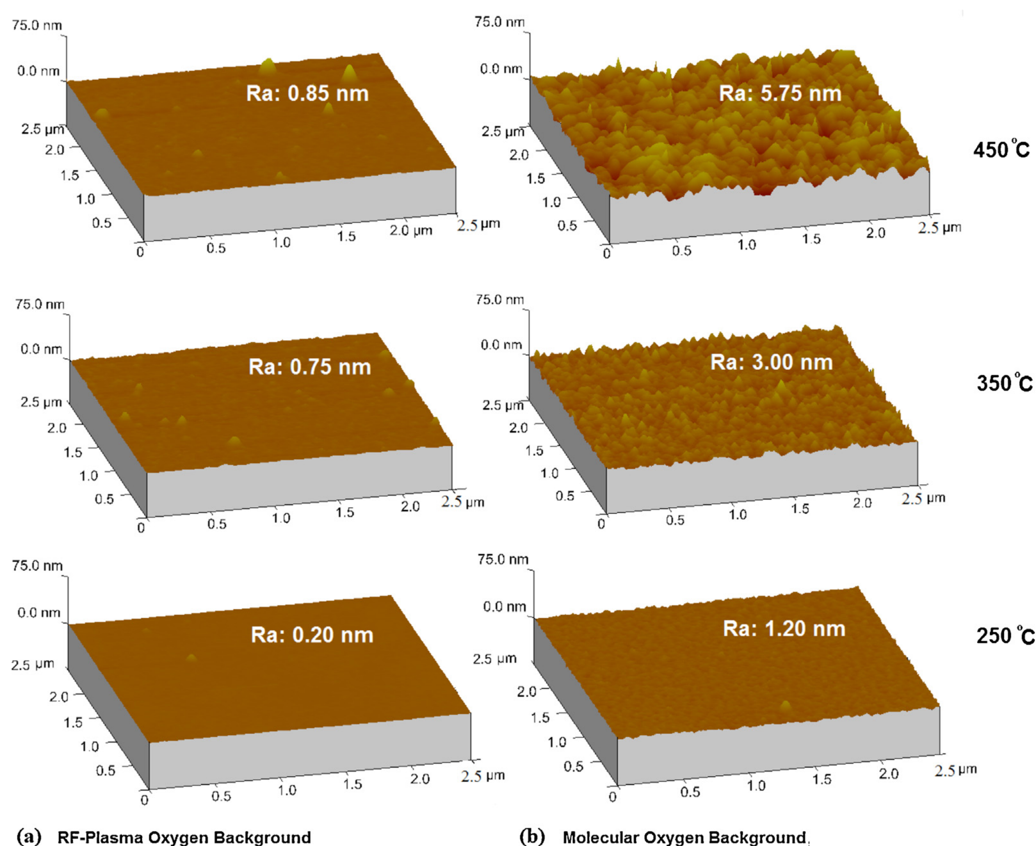

Fig. 3. AFM images for PLD grown CuO films, as a function of substrate temperature (250–450 °C) using two different PLD configurations, (a) R.F. plasma assisted background, (b) molecular gas background.

was imaged by AFM (Veeco multimode V Scan Probe Microscope) and the crystal structure and orientation of the films were investigated by XRD (PANalytical X'Pert X-ray Diffractometer equipped with a Ni filter and using Cu$K_{\alpha 1}$ radiation $\lambda = 1.5405$ A°). The electronic states of the films were investigated by XPS measurements. The optical properties and energy gap of each film were obtained from ellipsometery measurements and the electrical properties were determined using the conventional four probe conductivity measurements.

3. Results and discussion

3.1. Structural analysis

3.1.1. XRD

XRD patterns of CuO films deposited on MgO (1 0 0) substrates at different temperatures are shown in Fig. 2a for samples grown under R.F. plasma oxygen background, and Fig. 2b for samples grown under molecular oxygen background. Beside MgO (0 0 2) peak around $2\theta = 42°$, no other peaks except the peak located at $2\theta = 38.7°$, are observed, which correspond to (1 1 1) of CuO, suggesting single-phase CuO films are obtained. The needle-like spikes over the CuO (1 1 1) peaks are setup background and not associated to the CuO plane. The data shows highly textured (111) oriented CuO in both cases; but in R.F. plasma case, the peaks are prominent and more intensified indicating a better crystallinity. The increase in substrate heating of CuO samples of nearly same film thickness had a limited effect above 350 °C on the CuO (1 1 1) peak intensification in R.F. plasma case, while in the case of molecular background the peak is reduced at 450 °C.

3.1.2. AFM

AFM surface images (2.5 μm × 2.5 μm), depicting the surface morphologies of CuO films grown on MgO (1 0 0) at different temperatures, are illustrated in Fig. 3a for samples grown under R.F. plasma background, and Fig. 3b for samples grown under molecular oxygen background. Fig. 4 presents the root-mean-square (rms) values of average surface roughness of the samples. A huge

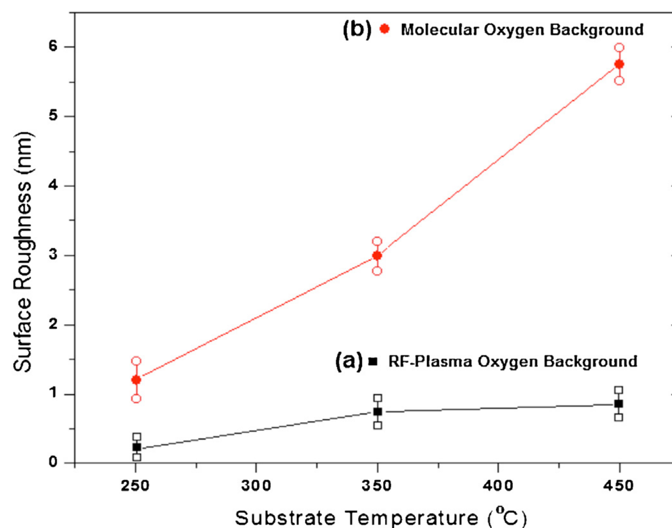

Fig. 4. Surface average roughness (Ra) recorded by AFM for PLD grown CuO films, as a function of substrate temperature (250–450 °C) using two different PLD configurations, (a) R.F. plasma assisted background, (b) molecular gas background.

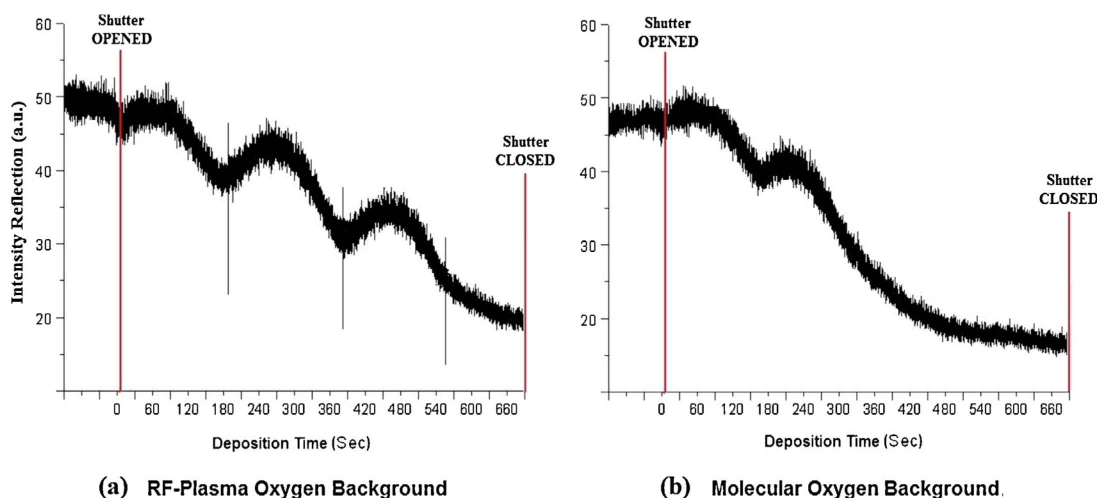

Fig. 5. RHEED intensity oscillations of two PLD grown CuO films at $T = 450\,^{\circ}$C and similar growth parameters using two different PLD configurations, (a) R.F. plasma assisted background, (b) molecular gas background.

improvement in surface morphology is observed by using R.F. plasma background (Fig. 3a and b). At one similar growth temperature the surface roughness is very different, and it is atomically smooth in the case of R.F. plasma background as confirmed by small rms values <1 nm (Fig. 4). Also it is observed that the average surface roughness of all samples is reduced while lowering the substrate temperature.

3.1.3. RHEED

Fig. 5 shows the RHEED-intensity variation during the growth of two CuO films grown at substrate temperature of 450 °C and growth rate of 0.022 A/laser pulse, equivalent to 0.054 unit cell/s. The growth rate of the grown films in this study is determined by temporal period of the RHEED intensity oscillations. Two different growth modes are distinguishable (Fig. 5a and b), as revealed by the two distinct characteristic RHEED profiles. The first growth mode is governed by the layer-by-layer growth up to three clearly identified oscillations (Fig. 5a), while the second changed to the 3D island mode after the first badly identified two unitcells (Fig. 5b). After 550 s of deposition, damped amplitude of the RHEED intensity oscillation is observed in both cases with the lack of intensity recovery.

3.1.4. XPS

XPS analyses were carried out on all samples using a VG-ESCALAB MK II Electron Spectrometer. The incident X-ray beam was produced by an aluminum anode (AlKα = 1486.6 eV). The C 1 s line of 284.6 eV binding energy was used as a reference to correct the binding energies for the charge shift. Fig. 6 (Cu2p) shows the Cu2p line of two samples prepared at $T = 450\,^{\circ}$C, under Oxygen RF Plasma and under molecular Oxygen atmosphere. The presence of the satellites of Cu2p3/2 and Cu2p1/2 is a finger print of the Cu^{2+} ions which confirms that the films are made of CuO phase in agreement with the XRD results. Fig. 7 shows the O1s spectra of two samples grown in different growth backgrounds but at same substrate temperature. The main peak located at 530 eV is assigned to the oxygen atoms of the CuO phase. The shoulder observed at higher binding energy side of the main peak (at about 532 eV) is related to moisture absorbed in the film [28]. It can be clearly noted that the relative ratio of moisture related to oxygen is less in the case of the sample prepared under RF plasma. This difference in moisture absorption can be related to the lower roughness of the surface of the RF sample as revealed by AFM images (Fig. 3). Table 1 shows the

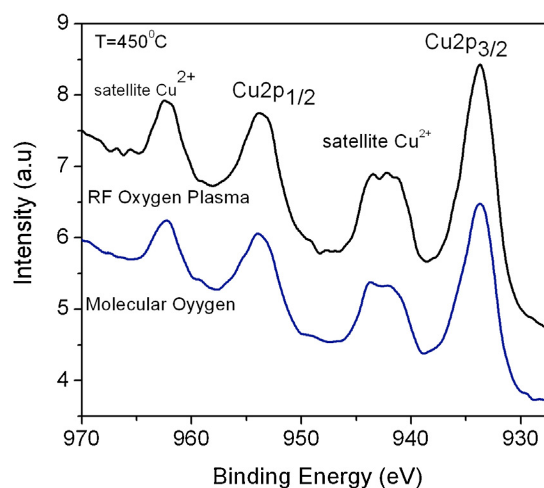

Fig. 6. Cu2p line of two CuO films prepared at $T = 450\,^{\circ}$C and similar growth conditions, under Oxygen RF Plasma and under molecular Oxygen background.

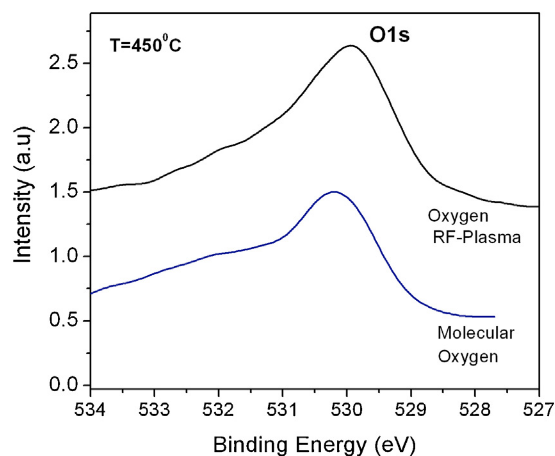

Fig. 7. O1s line line of two CuO films prepared at $T = 450\,^{\circ}$C and similar growth conditions. The main peak located at 530 eV binding energy is related to oxygen in CuO. The broad shoulder centered on 532 eV is assigned to moisture.

Table 1
The elemental composition and Cu:O ratio of CuO film grown at $T = 450\,^{\circ}\mathrm{C}$ and similar growth conditions, under Oxygen RF Plasma and under molecular Oxygen background.

Background	Normalized area			Ratio
	Cu2p3/2	Cu^{2+} satellite	O1s	O/Cu
RF-plasma	237	121	365	1.02
Molecular	168	82	267	1.07

elemental composition and Cu:O ratio of samples grown at 450 C. The composition of the films fluctuates slightly around the stoichiometric composition of CuO (O/Cu = 1), but it is closer to 1 in case of RF sample. This defines a better stoichiometric conservation of CuO phase during laser ablation in RF plasma background.

3.1.5. Discussion

The change in average surface roughness and CuO crystallinity with the growth temperature can be attributed to two factors. One is the CuO species diffusion length and the other is the interfacial reaction between CuO films and MgO substrates at different temperatures. On one hand, the higher temperature provides CuO species higher energy on the surface, which enables them to easily migrate on the substrate surface and has positive impact on the CuO growth, this correlates with XRD results. On the other hand, the higher temperature stimulates the interfacial reaction between the epilayer and the substrate, which reduces the as-grown CuO quality, as a result the surface morphology, this correlates with AFM data. With the decrease of the growth temperature, the interfacial reaction is significantly suppressed, this helps the growth quality. On the other hand the CuO species diffusion length becomes weaker but the kinetic energy provided by the laser can still make the species migrate effectively on the atomically flat MgO (1 0 0) surface. The improvement in structural quality of CuO films when using R.F. plasma background can be attributed to two factors. One is the CuO species gaining extra energy from the surrounding oxygen ions which are known to have greater momentum than neutral oxygen molecules, and the other is the activation of chemical reaction between CuO plume and the surrounding active oxygen species. Commonly in the two PLD configurations, the source of energy for the physical deposition is the interaction of laser with the electrons in the solid leading to a strong evaporative heating of the irradiated volume. The ablated material continuously absorbs energy from the laser, resulting in formation of an expanding energetic plasma plume up to several hundreds eV. After the termination of the laser pulse the plume expands adiabatically. In a background gas, the high plume pressure initially drives the expansion of species as if it were in vacuum. After several μs the plume propagation is completely determined by the interaction of plume energetic species with the constituents of background pressure. In case of R.F. plasma assisted PLD (Fig. 1a) the oxygen ionic beam ejected from the R.F. source and constituting the background pressure is much more kinetic than the neutral molecular oxygen background in case of standard PLD configuration (Fig. 1b). During a hyperthermal reaction, this background energy (up to 1000 eV) is added efficiently to the energies of the ablated CuO plume. Hence, in R.F. plasma assisted PLD the CuO species arrives at MgO surfaces with a relatively higher kinetic mobility compared to molecular oxygen case. This provides the species a longer diffusion length to locate in an energetically favorable lattice positions and helps to densify the film. Also it serves to maintain the thermodynamic stability of CuO phase. This elevation in surface kinetics replaces the need for substrate heating which motivates the interfacial reaction between CuO and MgO; therefore it doesn't deteriorate the crystal quality nor increase the surface roughness. On the other hand, R.F. plasma creates a higher concentration of oxygen ionic species

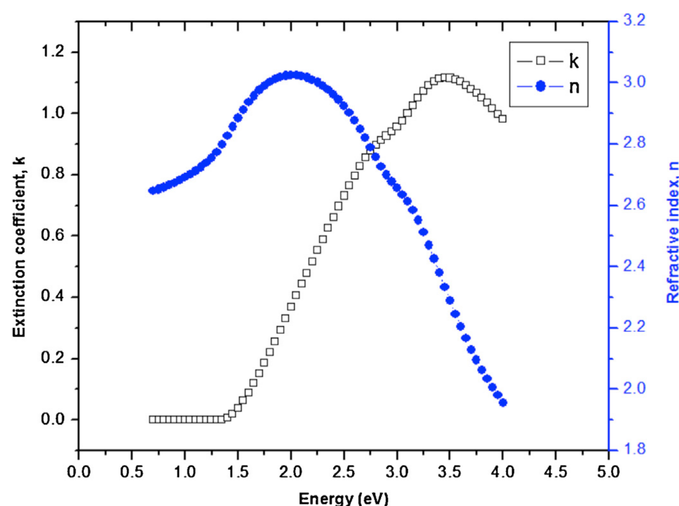

Fig. 8. The spectral distribution of refractive index and extinction coefficient of CuO film grown at $T = 450\,^{\circ}\mathrm{C}$.

or excited oxygen molecules interacting with the PLD plume as compared to molecular oxygen case. Such active oxygen rich environment enhances the conservation of CuO stoichiometric transfer from target to film at three positions. At the target side it compensates any oxygen loss during ablation, it rejoins any dissociated Cu atom inside the plume, also it reduces the probability of desorption of Cu species from the heated substrate. As a result this causes the incorporation of more CuO into the films as observed in XPS results. Oscillations in the RHEED specular intensity, clearly seen in R.F. plasma case, are an indication of the nucleation of 2D islands and their cyclical growth into flat terraces during layer-by-layer (Frank–van der Merwe) or the initial stages of layer-by-layer followed by island formation (Stranski–Krastanov) growth. In the case of molecular oxygen background the oscillations are fewer and weaker indicating that the growth was almost governed by 3D island formation mode (Volmer-Weber). This correlates with the difference in surface roughness observed in AFM of R.F. plasma and molecular gas samples.

3.2. Optoelectronic properties

Optoelectronic properties of best obtained CuO film, grown on MgO (1 0 0), at substrate temperature of 450 C, under 12×10^{-3} Pa oxygen R.F. plasma background, are presented in the following:

Ellipsometery measurements showed a display of light absorbance corresponding to photon energy. Fig. 8 presents the spectral distribution of refractive index, n and extinction coefficient, k. According to the equation: $(\alpha h\upsilon)^m = E_g - h\upsilon$, where E_g is the band gap, α is absorbance, h is Planck's constant, υ is the frequency, and m depends on the kind of optical transition that prevails. Specifically, m is 1/2 when the transition is indirect-allowed ($E_{g,ind}$), respectively [26,27]. The band gap is determined after rearrangements and necessary calculations were done. The resulting plot (Fig. 9) has distinct linear regimes which denote the onset of absorption. Thus, extrapolating these linear regions to the abscissa yields the energy of the optical band gap of the CuO film. The indirect band gap of the selected CuO film was found to be 1.32 eV.

Hall effect measurements were carried out at room temperature under 1.3 T magnetic field (Lakshore Instrument) and using van der Paw configuration. Gold contacts were deposited on the films by DC sputtering. The type of conductivity was confirmed from the sign of Hall coefficient. The different electrical parameters were found as follows: carriers of p-type, resistivity: 1.77 (Ω/cm), mobility: 36.7 $cm^2\,V^{-1}\,s^{-1}$, carrier concentration: $9.7 \times 10^{16}\,cm^{-3}$.

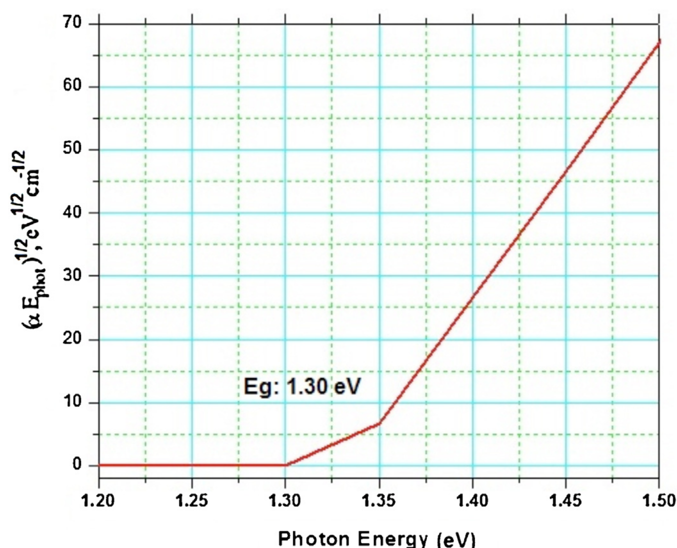

Fig. 9. Direct band gap of CuO film grown at $T = 450\,^{\circ}$C.

4. Conclusion

Cupric oxide (CuO) films were deposited on MgO (1 0 0) substrates to a similar thickness by two different pulsed laser deposition (PLD) configurations, molecular gas background and R.F. plasma assisted, at temperatures over 250–450 °C range. It is believed that, by XRD, AFM and RHEED analysis of the grown films, the energetic oxygen ions created by the R.F. plasma source and having greater momentum than neutral oxygen molecules, elevated the CuO plume kinetics and provided the mobile CuO species at MgO (1 0 0) surface longer diffusion lengths. This increased the possibility of the 2D growth mode and left the films highly textured in (1 1 1) direction and atomically smooth. On the other hand, the higher kinetics from the ionic background made the substrate heating of limited effect on the structural properties of the films grown in R.F. plasma assisted background but of a significant effect in the case of the molecular oxygen background. Moreover, the ionic background made the chemical reaction between CuO plume and the surrounding environment more preferable for a better stoichiometric transfer of CuO from target to film as observed in XPS data.

The optoelectronic properties obtained for a selected CuO film grown in R.F. plasma background match nicely the reported values in literature and are suitable for photovoltaic applications. In conclusion, we presented the advantages of using R.F. plasma assisted background for the laser ablation of CuO in comparison with the molecular oxygen background usually used in standard PLD configurations.

Acknowledgements

This work was supported by King Abdulaziz City for Science and Technology. The authors also thank Dr. Solomon Kolagani from NEOCERA Inc., USA, and Prof. Mahmoud Korek from Beirut Arab University, Lebanon and Prof. Malek Tabbal from American University of Beirut, Lebanon for the fruitful discussions.

References

[1] (a) Y.S. Chaudhary, A. Agrawal, R. Shrivastav, V.R. Satsangi, S. Dass, International Journal of Hydrogen Energy 29 (2004) 131–134;
(b) K.H. Yoon, W.J. Choi, D.H. Kang, Thin Solid Films 372 (2000) 250–256.
[2] T. Ito, H. Yamaguchi, T. Masumi, Journal of Materials Science 33 (1998) 3555–3566.
[3] D. Chauhan, V.R. Satsangi, S. Dass, R. Shrivastav, Bulletin of Materials Science 29 (2006) 709–716.
[4] Y.S. Chaudhary, A. Agrawal, R. Shrivastav, V.R. Satsangi, S. Dass, International Journal of Hydrogen Energy 29 (2004) 131.
[5] K.H. Yoon, W.J. Choi, D.H. Kang, Thin Solid Films 372 (2000) 250.
[6] M. Muhibbullah, M.O. Hakim, M.G.M. Choudhury, Thin Solid Films 423 (2003) 103.
[7] P. Nova'k, Electrochimica Acta 30 (1985) 1687.
[8] D.W. Kim, B. Park, J.H. Chung, K.S. Hong, Japanese Journal of Applied Physics 39 (2000) 2696.
[9] R.B. Vasiliev, M.N. Rumyantseva, N.V. Yakovlev, A.M. Gaskov, Sensors and Actuators B: Chemical 50 (1998) 186.
[10] Y. Nakamura, H. Zhuang, A. Kishimoto, O. Okada, H. Yanagida, Journal of the Electrochemical Society 145 (1998) 632.
[11] J.R. Ortiz, T. Ogura, J. Medina-Valtierra, S.E. Acosta-Ortiz, P. Bosh, J.A. de las Reyes, V.H. Lara, Applied Surface Science 174 (2001) 177.
[12] K.C.C. Kharas, Applied Catalysis B: Environmental 2 (1993) 207.
[13] L.C. Olsen, R.C. Bohara, Proc. 11th IEEE Photo. Spec. Conf. IEEE, New York, 1975, p. 381.
[14] D. Trivich, E.Y. Yang, R.J. Komp, A. Kakar, Proc. 13th IEEE Photo. Spec. Conf., New York, 1978, p. 174.
[15] C. Noguet, M. Tapiero, C. Schwab, J.P. Zielinger, D. Trivich, R.J. Komp, E.Y. Yang, K. Weng, Proceedings of the 1st Photo. Solar Energy Conference of the Commission of European Communities, Reidel, Dordrecht, 1977, p. 1170.
[16] N.A. Economu, R.S. Tech, R.J. Komp, D. Trivich, Proceedings of the 1st Photo. Solar Energy Conference of the Commission of European Communities, Reidel, Dordrecht, 1977, p. 1180.
[17] A. Catana, J.P. Locquet, S.M. Paik, I.K. Schuller, Physical Review 23 (1992) B46.
[18] V.P. Godbole, R.D. Vispute, S.M. Chaudhari, S.M. Kanetkar, S.B. Ogale, Journal of Materials Research 5 (1990) 372.
[19] R.K. Singh, J. Narayan, Physical Review B 41 (1990) 8843.
[20] K. Akimoto, S. Ishizuka, M. Yanagita, Y. Nawa, G.K. Paul, T. Sakurai, Solar Energy 80 (2006) 715–722.
[21] A. Chen, G. Yang, H. Long, F. Li, Y. Li, P. Lu, Thin Solid Films 517 (2009) 4277–4280.
[22] S.B. Ogale, P.G. Bilurkar, N. Mate, S.M. Kanetkar, N. Parikh, B. Patnaik, Journal of Applied of Physics 72 (1992) 3765.
[23] N. Kikuchi, K. Tonooka, Thin Solid Films 486 (2005) 33.
[24] J.-P. Locquet, Journal of the Less-Common Metals 300 (1990) 164–165.
[25] M. Kawwam, F. Alharbi, A. Aldwayyan, K. Lebbou, Applied Surface Science 24 (2012) 258.
[26] J.I. Pankove, Optical Processes in Semiconductors, Prentice-Hall, NJ, 1971, p. 340.
[27] J. Tauc, R. Grigorovici, A. Vancu, Physica Status Solidi 15 (1966) 627–637.
[28] I. Platzman, R. Brener, H. Haick, R. Tannenbaum, Journal of Physical Chemistry C 112 (2008) 1101–1108.